

# Splatting-based Synthesis for Video Frame Interpolation

Simon Niklaus  
Adobe Research

Ping Hu  
Boston University

Jiawen Chen  
Adobe Inc

## Abstract

Frame interpolation is an essential video processing technique that adjusts the temporal resolution of an image sequence. An effective approach to perform frame interpolation is based on splatting, also known as forward warping. Specifically, splatting can be used to warp the input images to an arbitrary temporal location based on an optical flow estimate. A synthesis network, also sometimes referred to as refinement network, can then be used to generate the output frame from the warped images. In doing so, it is common to not only warp the images but also various feature representations which provide rich contextual cues to the synthesis network. However, while this approach has been shown to work well and enables arbitrary-time interpolation due to using splatting, the involved synthesis network is prohibitively slow. In contrast, we propose to solely rely on splatting to synthesize the output without any subsequent refinement. This splatting-based synthesis is much faster than similar approaches, especially for multi-frame interpolation, while enabling new state-of-the-art results at high resolutions.

## 1. Introduction

Video frame interpolation is becoming more and more ubiquitous. While early techniques for frame interpolation were restricted to using block motion estimation and compensation due to performance constraints [8, 20], modern graphics accelerators allow for dense motion estimation and compensation while heavily making use of neural networks [37, 45, 46, 48]. These developments enable interesting new applications of video frame interpolation for animation inbetweening [32], video compression [63], video editing [40], motion blur synthesis [3], and many others.

However, existing interpolation techniques that heavily make use of neural networks are inherently difficult to accelerate. For example, the first interpolation approaches that use deep learning require fully executing the entire neural network for each output frame [37, 45, 46]. As such and as shown in Figure 1, using SepConv [46] (orange) to interpolate a given video by a factor of  $8\times$  instead of  $2\times$  requires

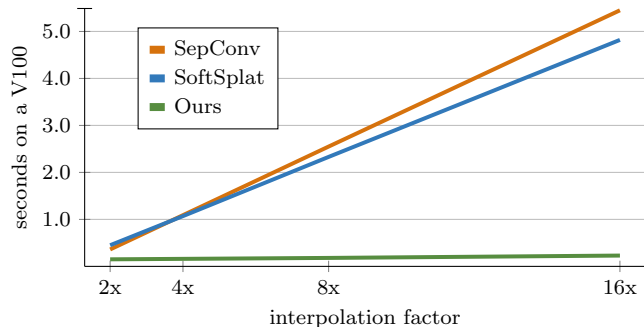


Figure 1. Runtime of two representative interpolation approaches versus our proposed one when interpolating multiple frames between two input images with a 2K resolution. Our approach interpolates the first frame in 148 milliseconds, each additional frame only takes a few milliseconds thanks to our splatting-based synthesis.

eight times more compute. Newer approaches are little different though. For example, SoftSplat [44] (blue) estimates the optical flow between the input frames and then warps feature pyramids to the desired interpolation instant before employing a synthesis network to yield the final result. While the optical flow only needs to be estimated once between two frames, the synthesis network has to be executed for each new frame which again requires roughly eight times more compute when interpolating by  $8\times$  instead of  $2\times$ .

To address such limitations, we propose a splatting-based synthesis approach. Specifically, we propose to solely rely on splatting to synthesize the output image without any subsequent refinement. As such, interpolating frames after estimating the optical flow requires only a few milliseconds and, as shown in Figure 1 (green), interpolating a given video by a factor of  $8\times$  instead of  $2\times$  requires hardly any more compute thanks to our image formation model. Further, our synthesis approach allows for the motion to be estimated at a lower resolution and to then upsample the estimated optical flow before using it to warp the input frames. This not only improves the computational efficiency, but counterintuitively can also lead to an improved interpolation quality.

The key to making our splatting-based synthesis approach work well is that it is carefully designed and that it is fully differentiable. Our careful design greatly improves the in-

method	venue	high-level summary
CtxSyn [43]	CVPR 2018	estimate $F_{0 \rightarrow 1}$ and $F_{1 \rightarrow 0}$ , extract features and splat them to time $t$ , synthesize the output $I_t$ using a neural network
Super SloMo [28]	CVPR 2018	estimate $F_{0 \rightarrow 1}$ and $F_{1 \rightarrow 0}$ , obtain $F_{t \rightarrow 0}$ and $F_{t \rightarrow 1}$ and visibilities using a network, backwarp and merge $I_0$ and $I_1$
DAIN [2]	CVPR 2019	estimate $F_{0 \rightarrow 1}$ and $F_{1 \rightarrow 0}$ , splat flows subject to $Z$ , extract and backwarp features to time $t$ , obtain $I_t$ using a network
SoftSplat [44]	CVPR 2020	estimate $F_{0 \rightarrow 1}$ and $F_{1 \rightarrow 0}$ , extract feature pyramids and splat them to time $t$ , synthesize $I_t$ using a neural network
EDSC [4]	arXiv 2020	estimate kernels as well as masks and offsets at $t$ using a network, apply deformable convolutions and merge the images
BMBC [50]	ECCV 2020	estimate $F_{t \rightarrow 0}$ and $F_{t \rightarrow 1}$ as well as $F_{0 \rightarrow 1}$ and $F_{1 \rightarrow 0}$ , extract features and splat them to $t$ , obtain $I_t$ using a network
AnimeInterp [32]	CVPR 2021	estimate coarse $F_{0 \rightarrow 1}$ and $F_{1 \rightarrow 0}$ , refine flows recurrently, extract feature and splat them, synthesize $I_t$ using a network
XVFI [57]	ICCV 2021	extract features, estimate $F_{0 \rightarrow 1}$ and $F_{1 \rightarrow 0}$ , splat flows and refine them, backwarp features and obtain $I_t$ using a network
Ours	N/A	estimate $F_{0 \rightarrow 1}$ and $F_{1 \rightarrow 0}$ , optionally upsample them, splat flows to get $F_{t \rightarrow 0}$ and $F_{t \rightarrow 1}$ , backwarp and merge $I_0$ and $I_1$

Table 1. Overview of recent video frame interpolation approaches that take two images as input and yield an interpolation result at an arbitrary time. For brevity we use the term features in the high-level summary to refer to various feature representations such as the input images themselves, contextual features, feature pyramids, depth maps, edge maps, occlusion masks, and visibility maps.

interpolation quality when compared to a common warping baseline (+1.35 dB on Vimeo-90k [66]), and being fully differentiable enables the underlying optical flow estimator to be fine-tuned which further improves the interpolation results (+1.43 dB on Vimeo-90k [66]). In short, we (1) identify a numerical instability in softmax splatting and propose an effective solution to address it, (2) introduce a splatting-based synthesis approach that is especially well-suited for multi-frame interpolation, and (3) show that iterative flow upsampling not only further improves the efficiency of our approach but can also lead to an improved quality.

## 2. Related Work

Warping-based video frame interpolation has a long history. Some examples based on block-level motion estimates include overlapping block motion compensation [8, 20], adaptively handling overlapping blocks [7], detecting and handling occlusions [24], considering multiple motion estimates [27], and estimating a dense motion field at the interpolation instant [12]. These are in contrast to motion compensation based on dense estimates which includes layered warping [54, 71], occlusion reasoning for temporal interpolation [22], warping with transition points [39], and using warping as a metric to evaluate optical flow [1].

Our proposed splatting-based synthesis is most closely related to warping techniques that leverage optical flow estimates while reasoning about occlusions [1, 22]. However, for a splatting-based synthesis approach to be used in a deep learning setting, the involved operations needs to be differentiable and easy to parallelize. This prohibits common techniques such as ordering and selecting a candidate flow in cases where multiple source pixels map to the same target [22], or iteratively filling holes [1]. In contrast, our proposed splatting-based synthesis technique only relies on differentiable operations that are easy to parallelize such as softmax splatting [44] and backward warping [26].

A common category of video frame interpolation approaches takes two images as input and interpolate a frame

at an arbitrary time  $t$  between the two inputs. We have summarized recent video frame interpolation techniques from this category in Table 1 since these are most closely related to our proposed synthesis approach. All of these methods have in common that they require running a neural network to infer the interpolation result at the desired instant. That is, they either use a neural network to refine warped representations of the input images, or use a neural network to infer the motion from the desired interpolation instant to the input images before accounting for it. Running such neural networks is computationally challenging though, especially at high resolutions. This is in contrast to our proposed splatting-based synthesis where, given optical flow estimates between the input frames, synthesizing the interpolation result at any time requires only a few primitive image operations.

Another category of video frame interpolation approaches takes two images as input and interpolate a frame at a fixed time, typically  $t = 0.5$ , between the two inputs. This includes kernel-based synthesis techniques [45, 46, 47], approaches that estimate the motion from the frame that is ought to be interpolated either implicitly [5, 31, 56] or explicitly [19, 36, 37, 51, 52, 68, 69], methods that directly synthesize the result [10, 29], and techniques that estimate the phase decomposition of the intermediate frame [41].

The area of video frame interpolation is much more diverse than these categories though. There is research on using more than two frames as input [6, 35, 55, 65], interpolating footage from event cameras [34, 60, 62, 67], efficient model design [10, 11, 13], test-time adaptation [9, 53], utilizing hybrid imaging systems [49], handling quantization artifacts [61], as well as joint deblurring [55] and joint super-resolution [30, 64]. Our proposed splatting-based synthesis technique is orthogonal to such research directions.

## 3. Stable Softmax Splatting

Our proposed synthesis approach is based on splatting, sometimes also referred to as forward warping. The challenge with splatting is that multiple pixels from the source

	Middlebury Baker <i>et al.</i> [1]		Vimeo-90k Xue <i>et al.</i> [66]		Xiph-1K (4K resized to 1K)		Xiph-2K (4K resized to 2K)		Xiph-4K (from xiph.org)	
	PSNR ↑	relative improvement	PSNR ↑	relative improvement	PSNR ↑	relative improvement	PSNR ↑	relative improvement	PSNR ↑	relative improvement
original SoftSplat [44]	38.42	–	36.10	–	37.96	–	36.62	–	34.20	–
with our stable softmax splatting	<u>38.59</u>	+ 0.17 dB	<u>36.18</u>	+ 0.08 dB	<u>37.99</u>	+ 0.03 dB	<u>36.74</u>	+ 0.12 dB	<u>34.62</u>	+ 0.42 dB

Table 2. Our stable softmax splatting formulation leads to subtle but consistent improvements when applied to the original SoftSplat [44].

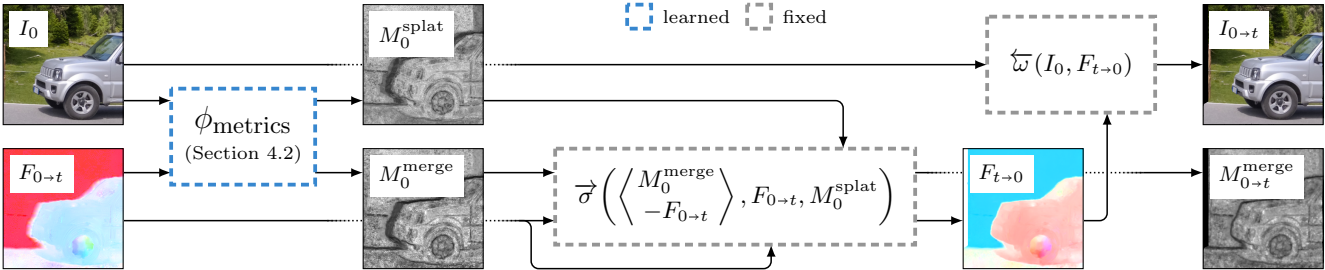


Figure 2. Overview of our splatting-based synthesis approach. In short, it takes an image  $I_0$  as well as an optical flow  $F_{0 \rightarrow t}$  and not only returns  $I_0$  warped to time  $t$  as  $I_{0 \rightarrow t}$  but also a weight map  $M_{0 \rightarrow t}^{\text{merge}}$  that can be used to merge multiple synthesis results. It leverages softmax splatting  $\vec{\sigma}$  [44] and backward warping  $\vec{\omega}$  [26] to do so. For frame interpolation, this approach needs to be applied twice, once for the forward direction as shown and once in the backward direction using  $I_1$  and  $F_{1 \rightarrow t}$ , before the individual results can be merged.

image can map to the same location in the target, which creates an ambiguity that in the context of deep learning needs to be resolved differentially. Softmax splatting is a recent solution to this problem [44], which has already found many applications [16, 17, 23, 33, 70]. However, we have found a numerical instability in the way softmax splatting is implemented, which we subsequently outline and address.

Given an image  $I_0$ , an optical flow  $F_{0 \rightarrow t}$  that maps pixels in  $I_0$  to the target time/location and a weight map  $Z_0$  to resolve ambiguities, softmax splatting  $\vec{\sigma}$  is defined as:

$$\vec{\sigma}(I_0, F_{0 \rightarrow t}, Z_0) = \frac{\vec{\Sigma}(\exp(Z_0) \cdot I_0, F_{0 \rightarrow t})}{\vec{\Sigma}(\exp(Z_0), F_{0 \rightarrow t})} \quad (1)$$

where  $\vec{\Sigma}(\cdot)$  is summation splatting [44] and  $Z_0$  is used to weight pixels in  $I_0$  to resolve cases where multiple pixels map to the same target location. This weight map  $Z_0$  can be thought of as an importance metric or as a soft inverse z-buffer (a hard z-buffer is not differentiable [42]).

The softmax operator is not usually implemented as defined since it is numerically unstable,  $\exp(X)$  quickly exceeds 32-bit floating point when  $X > 50$ . Fortunately, since  $\text{softmax}(X + c) = \text{softmax}(X)$  for any  $c$ , we can instead use  $\text{softmax}(X')$  where  $X' = X - \max(X)$  [18]. However, one cannot directly use this trick for softmax splatting. Consider a weight map  $Z_0$  with one element set to 1000 and all others  $\in [0, 1]$ . Shifting the weights by  $-1000$  effectively sets all but one weight to 0 and reduces the overall operation to average splatting, thus ignoring  $Z_0$  altogether.

The weights must be shifted adaptively at the destination where multiple source pixels overlap. As such, we first warp

$Z_0$  to time  $t$  as  $Z_{0 \rightarrow t}^{\max}$  which denotes the maximum weight for each pixel in the destination. This can be efficiently computed in parallel using an atomic max. Note that this step is and need not be differentiable as it is only used to make softmax splatting numerically stable. We can then subtract  $Z_{0 \rightarrow t}^{\max}[\mathbf{p}]$  from  $Z_0[\mathbf{q}]$  before applying the exponential function when warping from a point  $\mathbf{q}$  to  $\mathbf{p}$ , analogous to what is typically done when implementing softmax. We thus define our numerically stable softmax splatting as:

$$\text{let } \mathbf{u} = \mathbf{p} - (\mathbf{q} + F_{0 \rightarrow t}[\mathbf{q}]) \quad (2)$$

$$I_t[\mathbf{p}] = \frac{\sum_{\mathbf{q} \in I_0} b(\mathbf{u}) \cdot \exp(Z_0[\mathbf{q}] - Z_{0 \rightarrow t}^{\max}[\mathbf{p}]) \cdot I_0[\mathbf{q}]}{\sum_{\mathbf{q} \in I_0} b(\mathbf{u}) \cdot \exp(Z_0[\mathbf{q}] - Z_{0 \rightarrow t}^{\max}[\mathbf{p}])} \quad (3)$$

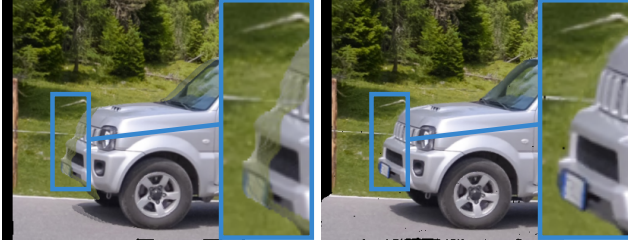
$$b(\mathbf{u}) = \max(0, 1 - |\mathbf{u}_x|) \cdot \max(0, 1 - |\mathbf{u}_y|). \quad (4)$$

where  $b(\cdot)$  is a bilinear kernel. Next, we demonstrate the benefits of this numerically stable implementation of softmax splatting on the task of video frame interpolation. As shown in Table 2, we reimplemented SoftSplat [44] and found that the enhanced numerical stability translates to subtle but consistent improvements in the interpolation quality. We expect similar improvements in other application domains.

## 4. Splatting-based Synthesis

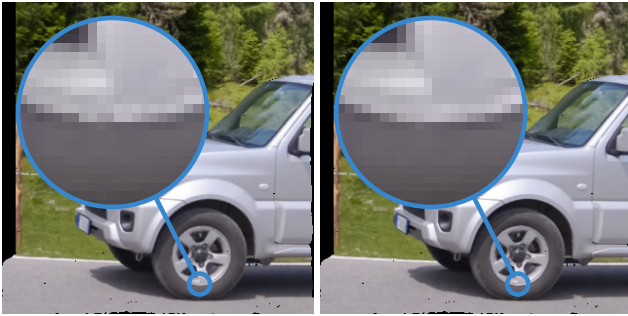
Our proposed splatting-based synthesis approach for video frame interpolation is summarized in Figure 2 and we will subsequently discuss its individual aspects. In doing so, we consider (1) how to resolve ambiguities where multiple pixels from the input image map to the same location





(a) naively splat  $I_0$  to get  $I_{0 \rightarrow t}$  (b) splatting weighted by  $M_0^{\text{splat}}$

Figure 3. We use a splatting metric  $M^{\text{splat}}$  that weights the individual pixels to resolve ambiguities where multiple pixels map to the same destination, thus properly handling occlusions.



(a) splat colors directly (b) splat flows then backward colors

Figure 4. Directly splatting the colors of an image can lead to subtle artifacts, which is why we splat flows instead and then synthesize the output using backwards warping of the splatted flows.

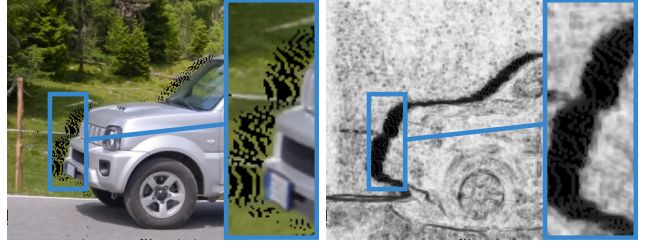
in the target, (2) how to do the warping without introducing any unnecessary artifacts, and for video frame interpolation in particular (3) how to merge  $I_0$  and  $I_1$  after warping them to synthesize the desired interpolation result  $I_t$  at time  $t$ .

#### 4.1. Splatting and Merging

The first step in our splatting-based synthesis for video frame interpolation is to warp  $I_0$  and  $I_1$  to the desired interpolation instant  $t$  using  $F_{0 \rightarrow t}$  and  $F_{1 \rightarrow t}$  respectively. However and as shown in Figure 3, one cannot simply splat an input image as is since multiple pixels in the source image may map to the same target location. To address this ambiguity, we follow recent work on softmax splatting [44] and use an auxiliary weight  $M^{\text{splat}}$  that serves as a soft inverse z-buffer. We will discuss how to compute  $M^{\text{splat}}$  in Section 4.2.

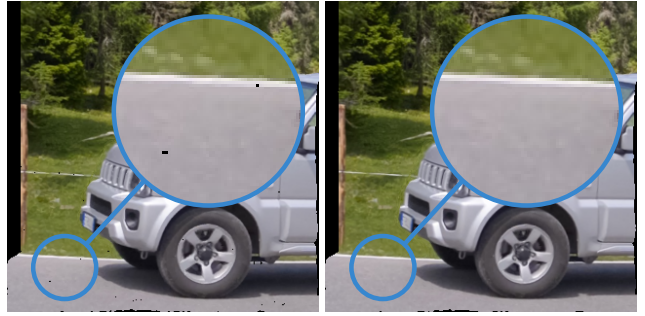
Next, one may be tempted to directly splat  $I_0$  using the optical flow  $F_{0 \rightarrow t}$  subject to the splatting metric  $M_0^{\text{splat}}$  in order to obtain  $I_{0 \rightarrow t}$  ( $I_0$  warped to time  $t$ ). However and as shown in Figure 4, this naive application of softmax splatting will lead to subtle artifacts and introduce unnecessary blurriness. Instead, we follow existing warping-based interpolation approaches and splat  $F_{0 \rightarrow t}$  to  $t$  to obtain  $F_{t \rightarrow 0}$  which is then used to backward warp  $I_0$  to  $t$  [1, 22].

Splatting naturally leads to holes in the warped result, due to not only occlusions but also divergent flow fields. As



(a) warped image  $I_{1 \rightarrow t}$  (b) corresponding  $M_{1 \rightarrow t}^{\text{merge}}$

Figure 5. We use a merging metric  $M^{\text{merge}}$  that weights the individual pixels in the warped images  $I_{0 \rightarrow t}$  and  $I_{1 \rightarrow t}$ , which suppresses the influence of unreliable pixels when generating  $I_t$ .



(a) splat flows with bilinear kernel (b) splat flows with Gaussian kernel

Figure 6. Splatting is subject to holes not only due to occlusions but also due to divergent flow fields, which we address by replacing the bilinear splatting kernel with a wider Gaussian kernel.

shown in Figure 6, splatting with a divergent flow results in small holes even in contiguous areas. To fill these holes, we replace the default bilinear splatting kernel, which only has a footprint of  $2 \times 2$ , with a  $4 \times 4$  Gaussian kernel. Note that such a wider kernel would lead to blurrier results when splatting colors, but it does not affect the clarity in our approach where we splat flows and then backward warp the image.

After these careful considerations we are able to faithfully warp  $I_0$  to  $I_{0 \rightarrow t}$  and  $I_1$  to  $I_{1 \rightarrow t}$ , but we cannot simply average these individual results to obtain the desired  $I_t$  since some pixels are more reliable than others as shown in Figure 5. As such, we introduce an auxiliary map  $M^{\text{merge}}$  that weights the individual results before merging them to obtain  $I_t$  as:

$$I_t = \frac{(1-t) \cdot M_{0 \rightarrow t}^{\text{merge}} \cdot I_{0 \rightarrow t} + t \cdot M_{1 \rightarrow t}^{\text{merge}} \cdot I_{1 \rightarrow t}}{(1-t) \cdot M_{0 \rightarrow t}^{\text{merge}} + t \cdot M_{1 \rightarrow t}^{\text{merge}}} \quad (5)$$

where  $I_{0 \rightarrow t}$  is  $I_0$  warped to time  $t$ ,  $M_{0 \rightarrow t}^{\text{splat}}$  is  $M_0^{\text{splat}}$  warped to time  $t$ , and analogous for  $I_{1 \rightarrow t}$  and  $M_{1 \rightarrow t}^{\text{splat}}$  in the opposite direction. We will subsequently describe how to obtain the involved splatting  $M^{\text{splat}}$  and merging  $M^{\text{merge}}$  metrics.

#### 4.2. Metrics for Splatting and Merging

Previous work on warping-based frame interpolation has successfully used photometric consistency to resolve the

	Middlebury Baker <i>et al.</i> [1]		Vimeo-90k Xue <i>et al.</i> [66]		Xiph-1K (4K resized to 1K)		Xiph-2K (4K resized to 2K)		Xiph-4K (from xiph.org)	
	PSNR ↑	relative improvement	PSNR ↑	relative improvement	PSNR ↑	relative improvement	PSNR ↑	relative improvement	PSNR ↑	relative improvement
fixed PWC-Net w/ [1] warping	33.80	–	32.22	–	33.61	–	33.59	–	32.61	–
fixed PWC-Net w/ our warping	34.73	+0.93 dB	33.57	+1.35 dB	35.03	+1.42 dB	34.90	+1.31 dB	33.66	+1.05 dB
tuned PWC-Net w/ our warping	<u>36.63</u>	+1.90 dB	<u>35.00</u>	+1.43 dB	<u>36.75</u>	+1.72 dB	<u>35.95</u>	+1.05 dB	<u>33.93</u>	+0.27 dB

Table 3. Comparing our splatting-based synthesis to a common warping-based interpolation technique [1]. Not only does our approach greatly outperform this baseline, it also allows us to fine-tune the utilized PWC-Net [58] which further improves the interpolation results.

splatting ambiguity where multiple source pixels map to the same location in the target [1]. This photometric consistency can be defined using backward warping  $\overleftarrow{\omega}(\cdot)$  as:

$$\psi_{\text{photo}} = \|I_0 - \overleftarrow{\omega}(I_1, F_{0 \rightarrow 1})\| \quad (6)$$

However, photometric consistency is easily affected by brightness changes, as is frequently the case with changes in shading. As such, we not only consider photometric consistency but also optical flow consistency defined as:

$$\psi_{\text{flow}} = \|F_{0 \rightarrow 1} + \overleftarrow{\omega}(F_{1 \rightarrow 0}, F_{0 \rightarrow 1})\| \quad (7)$$

Flow consistency is given if the flow of a pixel mapped to the target maps back to the pixel in the source, which is invariant to brightness changes and particularly useful for determining the  $M^{\text{splat}}$  metric. Another measure we consider is optical flow variance, which indicates local changes in flow as:

$$\psi_{\text{varia}} = \|\sqrt{G(F_{0 \rightarrow 1}^2) - G(F_{0 \rightarrow 1})^2}\| \quad (8)$$

where  $G(\cdot)$  denotes a  $3 \times 3$  Gaussian filter. Flow variance is high in areas with discontinuous flow, as is the case at motion boundaries. As shown in Figure 5, optical flow estimates tend to be inaccurate at boundaries which makes this measure particularly useful for the  $M^{\text{merge}}$  metric.

We conclude by combining these measures and define the splatting  $M^{\text{splat}}$  and merging  $M^{\text{merge}}$  metrics as:

$$M^{\text{splat}} = \frac{1}{1 + \alpha_p^s \cdot \psi_{\text{photo}}} + \frac{1}{1 + \alpha_f^s \cdot \psi_{\text{flow}}} + \frac{1}{1 + \alpha_v^s \cdot \psi_{\text{varia}}} \quad (9)$$

where  $\langle \alpha_p^s, \alpha_f^s, \alpha_v^s \rangle$  are tuneable parameters. The merge metric  $M^{\text{merge}}$  is defined analogous with  $\langle \alpha_p^m, \alpha_f^m, \alpha_v^m \rangle$ . We initially set these six parameters to 1 and learn their values through end-to-end training. We have also experimented with using a neural network to merge the individual measures, but have found Equation 9 to be faster and work better. Lastly, we also considered more complex measures such as depth estimates [2] but have found these not beneficial when also taking their computational complexity into account.

### 4.3. Baseline Comparison

We compare our proposed splatting-based synthesis for frame interpolation to a common warping-based interpolation technique [1] in Table 3, which shows that our approach

	Middlebury Baker <i>et al.</i> [1]		Vimeo-90k Xue <i>et al.</i> [66]	
	PSNR ↑	absolute deterioration	PSNR ↑	absolute deterioration
Ours	<u>36.63</u>	–	<u>35.00</u>	–
w/o flow splatting	36.27	-0.36 dB	34.86	-0.14 dB
w/o gaussian splatting	36.39	-0.24 dB	34.89	-0.11 dB
w/o stable splatting	36.48	-0.15 dB	34.97	-0.03 dB
w/o using $\psi_{\text{photo}}$	36.22	-0.41 dB	34.99	-0.01 dB
w/o using $\psi_{\text{flow}}$	36.44	-0.19 dB	34.99	-0.01 dB
w/o using $\psi_{\text{varia}}$	36.40	-0.23 dB	34.89	-0.11 dB

Table 4. Ablative experiments to analyze the design choices of our proposed splatting-based synthesis for video frame interpolation.

greatly outperforms this common baseline. However, since our image formation model is end-to-end differentiable, we can further improve the quality of our interpolated results by fine tuning the underlying optical flow estimator.

### 4.4. Ablative Experiments

We analyze the choices we made when designing our splatting-based synthesis for frame interpolation through ablative experiments. As shown in Table 4, each individual component contributes to the interpolation quality.

## 5. Iterative Flow Upsampling

It is impractical to compute optical flow on a 4K video. For high-resolution inputs, we thus propose to estimate the motion at a lower resolution and then use a neural network to iteratively upsample the optical flow to the full resolution of the input (see Figure 7). In practice, one may want to estimate the optical flow on either a 2K or a 1K resolution when given a 4K video depending on the desired performance characteristics. To support this use case, we subsequently propose an iterative flow upsampling approach.

### 5.1. Iterative Upsampling

We utilize a small neural network to perform iterative flow upsampling in an coarse-to-fine manner while using the high-resolution input frames as a guide. Specifically, given a flow estimate at a resolution of  $x$  as well as the

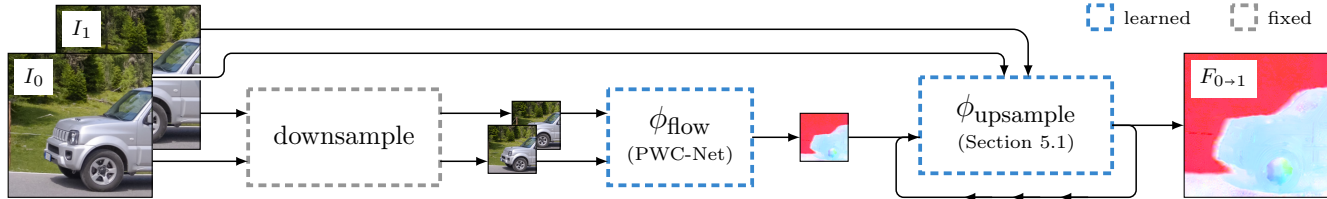


Figure 7. Overview of our iterative flow upsampling. Given two input images at a high resolution, we downsample them and then estimate the optical flow at a lower resolution. Our splatting-based synthesis requires flow estimates at the full resolution though, which is why we iteratively upsample the estimated flow guided by the input images (the more we downsampled, the more upsampling iterations we do).

	Middlebury Baker <i>et al.</i> [1]		Vimeo-90k Xue <i>et al.</i> [66]		Xiph-1K (4K resized to 1K)		Xiph-2K (4K resized to 2K)		Xiph-4K (from xiph.org)		runtime (seconds on a V100)		
	PSNR ↑	absolute rank	PSNR ↑	absolute rank	PSNR ↑	absolute rank	PSNR ↑	absolute rank	PSNR ↑	absolute rank	at 1K ↓	at 2K ↓	at 4K ↓
Ours w/o upsampling	36.63	1 <sup>st</sup> of 3	35.00	1 <sup>st</sup> of 3	36.75	1 <sup>st</sup> of 3	35.95	1 <sup>st</sup> of 3	33.93	3 <sup>rd</sup> of 3	0.043	0.148	0.589
Ours at 1/2 res. w/ 2× upsampling	34.79	2 <sup>nd</sup> of 3	33.89	2 <sup>nd</sup> of 3	35.37	2 <sup>nd</sup> of 3	35.52	2 <sup>nd</sup> of 3	<u>34.68</u>	1 <sup>st</sup> of 3	0.024	0.061	0.226
Ours at 1/4 res. w/ 4× upsampling	33.68	3 <sup>rd</sup> of 3	32.82	3 <sup>rd</sup> of 3	34.04	3 <sup>rd</sup> of 3	34.81	3 <sup>rd</sup> of 3	34.51	2 <sup>nd</sup> of 3	0.023	0.041	0.137

Table 5. Evaluating the effect of flow upsampling on the interpolation quality and the runtime. Counterintuitively, estimating the motion on a lower resolution is not only beneficial in terms of runtime, but sometimes also quality (see 1/2 res. w/ 2× upsampling on Xiph-4K).

two input images at a resolution of  $2 \cdot x$ , the upsampling network estimates the flow at a resolution of  $2 \cdot x$  through a sequence of four convolutions with PReLU [21] activations in between. To upsample a given flow estimate by a factor of  $4 \times$ , we execute this upsampling network twice.

We have found it beneficial to not only guide the upsampling by providing the input images, but also the three measures from Section 4.2 as they encode useful properties of the optical flow. We have otherwise kept our upsampling network deliberately simple without using spatially-varying upsampling kernels [59], normalized convolution upsampling [15], or self-guided upsampling [38]. After all, one of the reasons for estimating the flow at a lower resolution is improved efficiency and employing a more complex upsampling network would counteract this objective.

Another reason for estimating flow at a lower resolution is to mimic the inter-frame motion that the optical flow estimator was trained on during inference. In our implementation, we use PWC-Net [58] to estimate the optical flow and fine-tune it on input patches of size  $256 \times 256$  with a relatively small inter-frame motion magnitude. This flow estimator is expected to perform poorly on 4K inputs. But by down-sampling our inputs to resemble the data on which the flow estimation network was trained, we achieve a better frame interpolation result at high resolutions (see Table 5).

## 5.2. Baseline Comparison

We compare our proposed iterative flow upsampling to a baseline that only uses bilinear interpolation to upsample the flow in Figure 6, which shows that it is key to upsample the flow in a guided manner. Without a  $\phi_{\text{upsample}}$  trained specifically for this task, the drop in interpolation quality,

	Xiph-2K (4K resized to 2K)		Xiph-4K (from xiph.org)	
	PSNR ↑	relative improvement	PSNR ↑	relative improvement
at 1/2 res. w/ bilinear up.	34.91	–	34.51	–
at 1/2 res. w/ our up.	<u>35.52</u>	+ 0.61 dB	<u>34.68</u>	+ 0.17 dB
at 1/4 res. w/ bilinear up.	32.10	–	33.10	–
at 1/4 res. w/ our up.	34.81	+ 2.71 dB	34.51	+ 1.41 dB

Table 6. Comparison of our iterative flow upsampling with a baseline that only uses bilinear interpolation to upsample the flow.

especially when estimating the motion at 1/4 resolution and then upsampling it by a  $4 \times$ , would be too severe to usefully benefit from the improved computational efficiency.

## 6. Experiments

We subsequently provide additional implementation details, compare our proposed splatting-based synthesis for frame interpolation to other approaches, and discuss its limitations. Unless stated otherwise, we use our proposed interpolation pipeline without iterative flow upsampling on inputs of up to 2K and with  $2 \times$  down/upsampling for 4K inputs.

### 6.1. Implementation

We use PWC-Net [58] trained on FlyingChairs [14] as the basis for the underlying optical flow estimator  $\phi_{\text{flow}}$ . We fine-tune this flow estimator together with the six parameters of the metrics extractor  $\phi_{\text{metrics}}$  on the task of frame interpolation (Equation 5) with a laplacian loss [43] using crops of size  $256 \times 256$  from Vimeo-90k [66]. After convergence, we keep  $\phi_{\text{flow}}$  and  $\phi_{\text{metrics}}$  fixed while instead only training



venue		Middlebury Baker <i>et al.</i> [1]		Vimeo-90k Xue <i>et al.</i> [66]		Xiph-1K (4K resized to 1K)		Xiph-2K (4K resized to 2K)		Xiph-4K (from xiph.org)		runtime (seconds on a V100)		
		PSNR ↑	absolute rank	PSNR ↑	absolute rank	PSNR ↑	absolute rank	PSNR ↑	absolute rank	PSNR ↑	absolute rank	at 1K ↓	at 2K ↓	at 4K ↓
SepConv [46]	ICCV 2017	35.73	12 <sup>th</sup> of 16	33.80	14 <sup>th</sup> of 16	36.22	13 <sup>th</sup> of 16	34.77	13 <sup>th</sup> of 16	32.42	7 <sup>th</sup> of 16	0.096	0.321	1.245
CtxSyn [43]	CVPR 2018	36.93	7 <sup>th</sup> of 16	34.39	12 <sup>th</sup> of 16	36.87	5 <sup>th</sup> of 16	35.71	6 <sup>th</sup> of 16	33.85	4 <sup>th</sup> of 16	0.111	0.438	1.805
DAIN [2]	CVPR 2019	36.69	10 <sup>th</sup> of 16	34.70	10 <sup>th</sup> of 16	36.78	7 <sup>th</sup> of 16	35.93	5 <sup>th</sup> of 16	–	–	1.273	5.679	–
CAIN [10]	AAAI 2020	35.11	14 <sup>th</sup> of 16	34.65	11 <sup>th</sup> of 16	36.21	14 <sup>th</sup> of 16	35.18	9 <sup>th</sup> of 16	32.68	6 <sup>th</sup> of 16	0.047	0.158	0.597
EDSC <sub>s</sub> [4]	arXiv 2020	36.82	8 <sup>th</sup> of 16	34.83	8 <sup>th</sup> of 16	36.73	9 <sup>th</sup> of 16	34.81	12 <sup>th</sup> of 16	–	–	0.961	1.334	–
EDSC <sub>m</sub> [4]	arXiv 2020	34.37	15 <sup>th</sup> of 16	33.34	15 <sup>th</sup> of 16	35.29	15 <sup>th</sup> of 16	34.62	16 <sup>th</sup> of 16	–	–	0.961	1.334	–
AdaCoF [31]	CVPR 2020	35.72	13 <sup>th</sup> of 16	34.35	13 <sup>th</sup> of 16	36.26	12 <sup>th</sup> of 16	34.82	11 <sup>th</sup> of 16	32.12	9 <sup>th</sup> of 16	0.033	0.125	0.499
SoftSplat [44]	CVPR 2020	<u>38.42</u>	1 <sup>st</sup> of 16	36.10	2 <sup>nd</sup> of 16	<u>37.96</u>	1 <sup>st</sup> of 16	<u>36.62</u>	1 <sup>st</sup> of 16	34.20	2 <sup>nd</sup> of 16	0.117	0.444	1.768
BMBC [50]	ECCV 2020	36.79	9 <sup>th</sup> of 16	35.06	6 <sup>th</sup> of 16	36.59	10 <sup>th</sup> of 16	34.67	15 <sup>th</sup> of 16	–	–	1.139	4.398	–
RIFE [25]	arXiv 2020	37.30	3 <sup>rd</sup> of 16	35.61	3 <sup>rd</sup> of 16	37.38	2 <sup>nd</sup> of 16	36.16	3 <sup>rd</sup> of 16	33.47	5 <sup>th</sup> of 16	0.017	0.058	0.317
SepConv++ [47]	WACV 2021	37.28	4 <sup>th</sup> of 16	34.83	8 <sup>th</sup> of 16	36.83	6 <sup>th</sup> of 16	34.84	10 <sup>th</sup> of 16	32.23	8 <sup>th</sup> of 16	0.092	0.364	1.455
CDFI [13]	CVPR 2021	37.14	5 <sup>th</sup> of 16	35.17	4 <sup>th</sup> of 16	37.05	3 <sup>rd</sup> of 16	35.46	7 <sup>th</sup> of 16	–	–	0.230	0.916	–
XVFI [57]	ICCV 2021	33.27	16 <sup>th</sup> of 16	32.49	16 <sup>th</sup> of 16	34.54	16 <sup>th</sup> of 16	34.76	14 <sup>th</sup> of 16	33.99	3 <sup>rd</sup> of 16	0.114	0.297	0.964
XVFI <sub>v</sub> [57]	ICCV 2021	37.09	6 <sup>th</sup> of 16	35.07	5 <sup>th</sup> of 16	36.98	4 <sup>th</sup> of 16	35.19	8 <sup>th</sup> of 16	32.12	9 <sup>th</sup> of 16	0.114	0.297	0.964
ABME [51]	ICCV 2021	37.64	2 <sup>nd</sup> of 16	<u>36.18</u>	1 <sup>st</sup> of 16	36.53	11 <sup>th</sup> of 16	36.50	2 <sup>nd</sup> of 16	–	–	0.336	1.057	–
Ours	N/A	36.63	11 <sup>th</sup> of 16	35.00	7 <sup>th</sup> of 16	36.75	8 <sup>th</sup> of 16	35.95	4 <sup>th</sup> of 16	<u>34.68</u>	1 <sup>st</sup> of 16	0.043	0.148	0.226

Table 7. Quantitative comparison of our proposed approach with various recent frame interpolation techniques that operate on two input images. The higher the resolution the better our approach ranks, and it performs best on the Xiph-4K test where it is also the fastest.

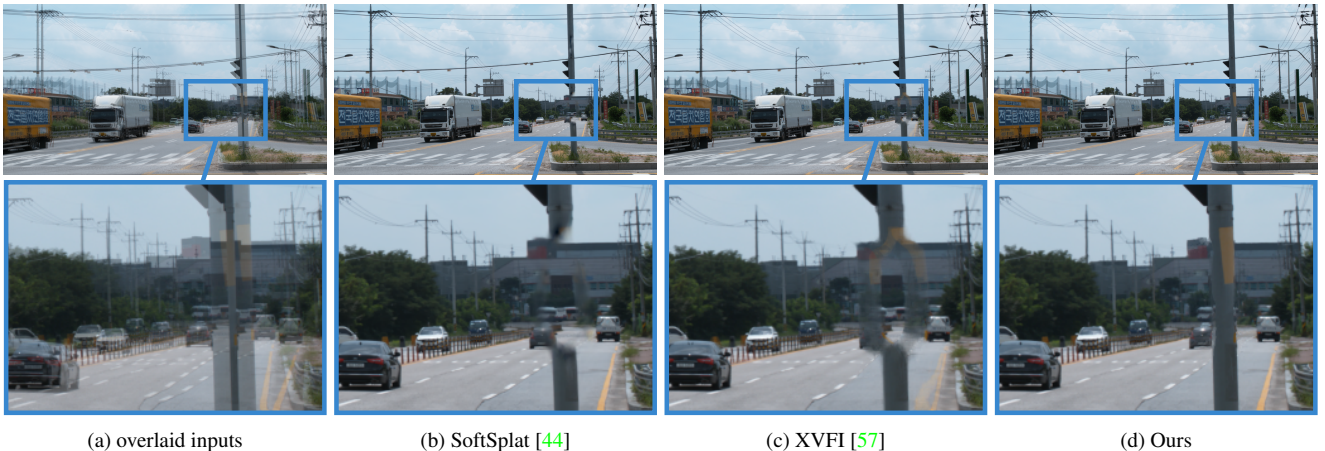


Figure 8. Qualitative comparison of our proposed approach with two representative methods on a sample from the XTEST-2K [57] test dataset. While these sophisticated interpolation methods are unable to handle this challenging scenario with the utility pole subject to large motion, our comparatively simple approach is able to generate a plausible result. Please consider our supplementary for more results.

the iterative flow upsampling network  $\phi_{\text{upsample}}$ , again using crops from the Vimeo-90k dataset. However, this time we uniformly sample the crop width from  $\mathcal{U}(192, 448)$  and the crop height from  $\mathcal{U}(192, 256)$  such that the upsampling network is supervised on various aspect ratios. During training, we run  $\phi_{\text{upsample}}$  randomly for either one or two iterations.

## 6.2. Quantitative Evaluation

We quantitatively evaluate our splatting-based frame interpolation approach on common benchmark datasets, which includes the samples from the Middlebury benchmark with public ground truth [1], the test split of the Vimeo-90k

dataset [66], as well as samples from Xiph [44]. For brevity, we follow recent work and focus on the peak signal-to-noise ratio [47]. We compare our approach to a plethora of other frame interpolation methods that take two images as input.

As shown in Table 7, the higher the resolution the better our approach ranks and it performs best on Xiph-4K where it is also the fastest. While our approach does not perform too well on low resolutions like with the Middlebury samples and the Vimeo-90k test split, it is surprising that it outperforms both CtxSyn [43] and DAIN [2] on the latter. After all, these methods not only splat the input images but also various feature representations before employing a synthesis network

	XTEST-1K (4K resized to 1K)		XTEST-2K (4K resized to 2K)		XTEST-4K Sim <i>et al.</i> [57]	
	PSNR ↑	absolute rank	PSNR ↑	absolute rank	PSNR ↑	absolute rank
SepConv [46]	30.35	8 <sup>th</sup> of 16	26.60	10 <sup>th</sup> of 16	24.32	8 <sup>th</sup> of 16
CtxSyn [43]	31.92	5 <sup>th</sup> of 16	29.12	6 <sup>th</sup> of 16	25.46	4 <sup>th</sup> of 16
DAIN [2]	32.51	3 <sup>rd</sup> of 16	31.49	2 <sup>nd</sup> of 16	—	—
CAIN [10]	30.23	10 <sup>th</sup> of 16	26.72	9 <sup>th</sup> of 16	24.50	5 <sup>th</sup> of 16
EDSC <sub>s</sub> [4]	30.54	7 <sup>th</sup> of 16	26.37	11 <sup>th</sup> of 16	—	—
EDSC <sub>m</sub> [4]	29.62	13 <sup>th</sup> of 16	27.45	7 <sup>th</sup> of 16	—	—
AdaCoF [31]	28.69	14 <sup>th</sup> of 16	26.20	12 <sup>th</sup> of 16	24.36	6 <sup>th</sup> of 16
SoftSplat [44]	<u>33.42</u>	1 <sup>st</sup> of 16	29.73	5 <sup>th</sup> of 16	25.48	3 <sup>rd</sup> of 16
BMBC [50]	30.04	11 <sup>th</sup> of 16	25.46	14 <sup>th</sup> of 16	—	—
RIFE [25]	23.61	16 <sup>th</sup> of 16	22.79	16 <sup>th</sup> of 16	22.18	10 <sup>th</sup> of 16
SepConv++ [47]	29.78	12 <sup>th</sup> of 16	26.12	13 <sup>th</sup> of 16	24.36	6 <sup>th</sup> of 16
CDFI [13]	30.30	9 <sup>th</sup> of 16	26.89	8 <sup>th</sup> of 16	—	—
XVFI [57]	31.54	6 <sup>th</sup> of 16	31.12	3 <sup>rd</sup> of 16	30.12	2 <sup>nd</sup> of 16
XVFI <sub>v</sub> [57]	26.91	15 <sup>th</sup> of 16	24.49	15 <sup>th</sup> of 16	22.83	9 <sup>th</sup> of 16
ABME [51]	32.08	4 <sup>th</sup> of 16	30.15	4 <sup>th</sup> of 16	—	—
Ours	33.31	2 <sup>nd</sup> of 16	<u>32.27</u>	1 <sup>st</sup> of 16	<u>31.34</u>	1 <sup>st</sup> of 16

Table 8. Evaluating the  $8\times$  interpolation ability of our approach in comparison to various other techniques on XTEST [57].

to generate the result. In contrast, our synthesis is purely based on splatting without any subsequent refinement.

### 6.3. Qualitative Evaluation

Video frame interpolation results are best viewed as a motion picture, which is why we limit the qualitative evaluation in our main paper to only a single example in Figure 8 and kindly refer to our supplementary for more results.

### 6.4. Multi-frame Interpolation

One of the benefits of our splatting-based synthesis is that once the motion has been estimated, interpolating frames only takes a few milliseconds. This makes our technique particularly useful for multi-frame interpolation, which we evaluate using the XTEST [57] benchmark. Since we have found the inter-frame motion in this dataset to be rather extreme as its name suggests, we use our proposed approach with iterative  $2\times$  down/upsampling on 2K inputs while using iterative  $4\times$  down/upsampling on 4K inputs.

The results of this evaluation are shown in Table 8 and we analyze per-frame metrics in Figure 9. Our approach performs particularly well on XTEST, which we attribute to its favorable ability to handle large motion. Furthermore, the per-frame analysis shows that our splatting-based synthesis is temporally consistent and highly efficient when synthesizing multiple frames between two given ones at once.

### 6.5. Limitations

While generating results with our splatting-based synthesis is fast, it is wholly relying on the quality of the underlying

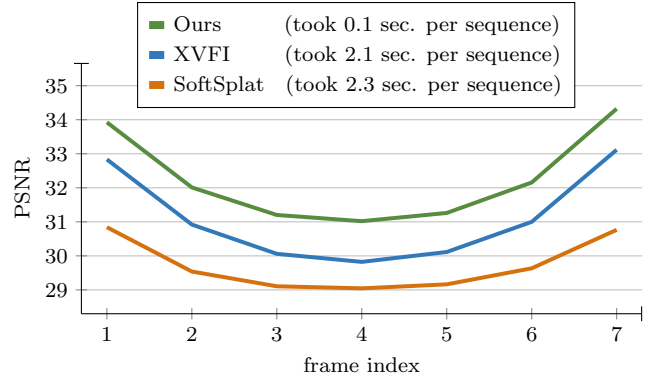


Figure 9. Evaluating the per-frame quality when performing  $8\times$  interpolation on XTEST-2K [57]. Our proposed approach not only generates better results, it also does so an order of magnitude faster thanks to our splatting-based synthesis technique which is particularly well-suited for interpolating multiple frames at once.

optical flow estimate. In contrast, the refinement network that is used in related approaches that splat features before synthesizing the output using the warped features is able to account for minor inaccuracies in the estimated motion. Similarly, our splatting-based synthesis requires all the information that is necessary to interpolate the intermediate frame to be present in the input. However, this may not always be the case due to occlusions. In contrast, approaches with a refinement network can hallucinate missing content.

## 7. Conclusion

In this paper, we show how to perform video frame interpolation while synthesizing the output solely through splatting. As such, synthesizing a frame only takes a few milliseconds once the inter-frame motion has been estimated, which makes our approach particularly useful for multi-frame interpolation. Furthermore, we combine this splatting-based synthesis approach with an iterative flow upsampling scheme which not only benefits the computational efficiency but also improves the interpolation quality at high resolutions.

## References

- [1] Simon Baker, Daniel Scharstein, J. P. Lewis, Stefan Roth, Michael J. Black, and Richard Szeliski. A Database and Evaluation Methodology for Optical Flow. *International Journal of Computer Vision*, 92(1):1–31, 2011. 2, 3, 4, 5, 6, 7
- [2] Wenbo Bao, Wei-Sheng Lai, Chao Ma, Xiaoyun Zhang, Zhiyong Gao, and Ming-Hsuan Yang. Depth-Aware Video Frame Interpolation. In *IEEE Conference on Computer Vision and Pattern Recognition*, 2019. 2, 5, 7, 8
- [3] Tim Brooks and Jonathan T. Barron. Learning to Synthesize Motion Blur. In *IEEE Conference on Computer Vision and Pattern Recognition*, 2019. 1
- [4] Xianhang Cheng and Zhenzhong Chen. Multiple Video Frame Interpolation via Enhanced Deformable Separable Convolution. *arXiv/2006.08070*, 2020. 2, 7, 8



- [5] Xianhang Cheng and Zhenzhong Chen. Video Frame Interpolation via Deformable Separable Convolution. In *AAAI Conference on Artificial Intelligence*, 2020. 2
- [6] Zhixiang Chi, Rasoul Mohammadi Nasiri, Zheng Liu, Juwei Lu, Jin Tang, and Konstantinos N. Plataniotis. All at Once: Temporally Adaptive Multi-Frame Interpolation With Advanced Motion Modeling. In *European Conference on Computer Vision*, 2020. 2
- [7] Byeong-Doo Choi, Jong-Woo Han, Chang-Su Kim, and Sung-Jea Ko. Motion-Compensated Frame Interpolation Using Bilateral Motion Estimation and Adaptive Overlapped Block Motion Compensation. *IEEE Transactions on Circuits and Systems for Video Technology*, 17(4):407–416, 2007. 2
- [8] Byung-Tae Choi, Sung-Hee Lee, and Sung-Jea Ko. New Frame Rate Up-Conversion Using Bi-Directional Motion Estimation. *IEEE Transactions on Consumer Electronics*, 46(3):603–609, 2000. 1, 2
- [9] Myungsub Choi, Janghoon Choi, Sungyong Baik, Tae Hyun Kim, and Kyoung Mu Lee. Scene-Adaptive Video Frame Interpolation via Meta-Learning. In *IEEE Conference on Computer Vision and Pattern Recognition*, 2020. 2
- [10] Myungsub Choi, Heewon Kim, Bohyung Han, Ning Xu, and Kyoung Mu Lee. Channel Attention Is All You Need for Video Frame Interpolation. In *AAAI Conference on Artificial Intelligence*, 2020. 2, 7, 8
- [11] Myungsub Choi, Suyoung Lee, Heewon Kim, and Kyoung Mu Lee. Motion-Aware Dynamic Architecture for Efficient Frame Interpolation. In *IEEE International Conference on Computer Vision*, 2021. 2
- [12] Salih Dikbas and Yucl Altunbasak. Novel True-Motion Estimation Algorithm and Its Application to Motion-Compensated Temporal Frame Interpolation. *IEEE Transactions on Image Processing*, 22(8):2931–2945, 2013. 2
- [13] Tianyu Ding, Luming Liang, Zhihui Zhu, and Ilya Zharkov. CDFI: Compression-Driven Network Design for Frame Interpolation. In *IEEE Conference on Computer Vision and Pattern Recognition*, 2021. 2, 7, 8
- [14] Alexey Dosovitskiy, Philipp Fischer, Eddy Ilg, Philip Häusser, Caner Hazirbas, Vladimir Golkov, Patrick van der Smagt, Daniel Cremers, and Thomas Brox. FlowNet: Learning Optical Flow With Convolutional Networks. In *IEEE International Conference on Computer Vision*, 2015. 6
- [15] Abdelrahman Eldesokey and Michael Felsberg. Normalized Convolution Upsampling for Refined Optical Flow Estimation. *arXiv/2102.06979*, 2021. 6
- [16] Bin Fan and Yuchao Dai. Inverting a Rolling Shutter Camera: Bring Rolling Shutter Images to High Framerate Global Shutter Video. In *IEEE International Conference on Computer Vision*, 2021. 3
- [17] Runsen Feng, Zongyu Guo, Zhizheng Zhang, and Zhibo Chen. Versatile Learned Video Compression. *arXiv/2111.03386*, 2021. 3
- [18] Ian Goodfellow, Yoshua Bengio, and Aaron Courville. *Deep Learning*. MIT Press, 2016. 3
- [19] Shurui Gui, Chaoyue Wang, Qihua Chen, and Dacheng Tao. FeatureFlow: Robust Video Interpolation via Structure-to-Texture Generation. In *IEEE Conference on Computer Vision and Pattern Recognition*, 2020. 2
- [20] Taehyeun Ha, Seongjoo Lee, and Jaeseok Kim. Motion Compensated Frame Interpolation by New Block-Based Motion Estimation Algorithm. *IEEE Transactions on Consumer Electronics*, 50(2):752–759, 2004. 1, 2
- [21] Kaiming He, Xiangyu Zhang, Shaoqing Ren, and Jian Sun. Delving Deep Into Rectifiers: Surpassing Human-Level Performance on ImageNet Classification. In *IEEE International Conference on Computer Vision*, 2015. 6
- [22] Evan Herbst, Steve Seitz, and Simon Baker. Occlusion Reasoning for Temporal Interpolation Using Optical Flow. Technical report, 2009. 2, 4
- [23] Aleksander Holynski, Brian L. Curless, Steven M. Seitz, and Richard Szeliski. Animating Pictures With Eulerian Motion Fields. In *IEEE Conference on Computer Vision and Pattern Recognition*, 2021. 3
- [24] Ai-Mei Huang and Truong Q. Nguyen. Correlation-Based Motion Vector Processing With Adaptive Interpolation Scheme for Motion-Compensated Frame Interpolation. *IEEE Transactions on Image Processing*, 18(4):740–752, 2009. 2
- [25] Zhewei Huang, Tianyuan Zhang, Wen Heng, Boxin Shi, and Shuchang Zhou. RIFE: Real-Time Intermediate Flow Estimation for Video Frame Interpolation. *arXiv/2011.06294*, 2020. 7, 8
- [26] Max Jaderberg, Karen Simonyan, Andrew Zisserman, and Koray Kavukcuoglu. Spatial Transformer Networks. In *Advances in Neural Information Processing Systems*, 2015. 2, 3
- [27] Seong-Gyun Jeong, Chul Lee, and Chang-Su Kim. Motion-Compensated Frame Interpolation Based on Multihypothesis Motion Estimation and Texture Optimization. *IEEE Transactions on Image Processing*, 22(11):4497–4509, 2013. 2
- [28] Huaizu Jiang, Deqing Sun, Varun Jampani, Ming-Hsuan Yang, Erik G. Learned-Miller, and Jan Kautz. Super SloMo: High Quality Estimation of Multiple Intermediate Frames for Video Interpolation. In *IEEE Conference on Computer Vision and Pattern Recognition*, 2018. 2
- [29] Tarun Kalluri, Deepak Pathak, Manmohan Chandraker, and Du Tran. FLAVR: Flow-Agnostic Video Representations for Fast Frame Interpolation. *arXiv/2012.08512*, 2020. 2
- [30] Soo Ye Kim, Jihyong Oh, and Munchurl Kim. FISR: Deep Joint Frame Interpolation and Super-Resolution With a Multi-Scale Temporal Loss. In *AAAI Conference on Artificial Intelligence*, 2020. 2
- [31] Hyeongmin Lee, Taeoh Kim, Tae-Young Chung, Daehyun Pak, Yuseok Ban, and Sangyoun Lee. AdaCoF: Adaptive Collaboration of Flows for Video Frame Interpolation. In *IEEE Conference on Computer Vision and Pattern Recognition*, 2020. 2, 7, 8
- [32] Siyao Li, Shiyu Zhao, Weijiang Yu, Wenxiu Sun, Dimitris N. Metaxas, Chen Change Loy, and Ziwei Liu. Deep Animation Video Interpolation in the Wild. In *IEEE Conference on Computer Vision and Pattern Recognition*, 2021. 1, 2
- [33] Zhengqi Li, Simon Niklaus, Noah Snavely, and Oliver Wang. Neural Scene Flow Fields for Space-Time View Synthesis of Dynamic Scenes. In *IEEE Conference on Computer Vision and Pattern Recognition*, 2021. 3
- [34] Songnan Lin, Jiawei Zhang, Jinshan Pan, Zhe Jiang, Dongqing Zou, Yongtian Wang, Jing Chen, and Jimmy S. J.

- Ren. Learning Event-Driven Video Deblurring and Interpolation. In *European Conference on Computer Vision*, 2020. 2
- [35] Yihao Liu, Liangbin Xie, Siyao Li, Wenxiu Sun, Yu Qiao, and Chao Dong. Enhanced Quadratic Video Interpolation. *arXiv/2009.04642*, 2020. 2
- [36] Yu-Lun Liu, Yi-Tung Liao, Yen-Yu Lin, and Yung-Yu Chuang. Deep Video Frame Interpolation Using Cyclic Frame Generation. In *AAAI Conference on Artificial Intelligence*, 2019. 2
- [37] Ziwei Liu, Raymond A. Yeh, Xiaoou Tang, Yiming Liu, and Aseem Agarwala. Video Frame Synthesis Using Deep Voxel Flow. In *IEEE International Conference on Computer Vision*, 2017. 1, 2
- [38] Kunming Luo, Chuan Wang, Shuaicheng Liu, Haoqiang Fan, Jue Wang, and Jian Sun. UPFlow: Upsampling Pyramid for Unsupervised Optical Flow Learning. In *IEEE Conference on Computer Vision and Pattern Recognition*, 2021. 6
- [39] Dhruv Mahajan, Fu-Chung Huang, Wojciech Matusik, Ravi Ramamoorthi, and Peter N. Belhumeur. Moving Gradients: A Path-Based Method for Plausible Image Interpolation. *ACM Transactions on Graphics*, 28(3):42:1–42:11, 2009. 2
- [40] Simone Meyer, Victor Cornillère, Abdelaziz Djelouah, Christopher Schroers, and Markus H. Gross. Deep Video Color Propagation. In *British Machine Vision Conference*, 2018. 1
- [41] Simone Meyer, Abdelaziz Djelouah, Brian McWilliams, Alexander Sorkine-Hornung, Markus H. Gross, and Christopher Schroers. PhaseNet for Video Frame Interpolation. In *IEEE Conference on Computer Vision and Pattern Recognition*, 2018. 2
- [42] Thu Nguyen-Phuoc, Chuan Li, Stephen Balaban, and Yong-Liang Yang. RenderNet: A Deep Convolutional Network for Differentiable Rendering From 3D Shapes. In *Advances in Neural Information Processing Systems*, 2018. 3
- [43] Simon Niklaus and Feng Liu. Context-Aware Synthesis for Video Frame Interpolation. In *IEEE Conference on Computer Vision and Pattern Recognition*, 2018. 2, 6, 7, 8
- [44] Simon Niklaus and Feng Liu. Softmax Splatting for Video Frame Interpolation. In *IEEE Conference on Computer Vision and Pattern Recognition*, 2020. 1, 2, 3, 4, 7, 8
- [45] Simon Niklaus, Long Mai, and Feng Liu. Video Frame Interpolation via Adaptive Convolution. In *IEEE Conference on Computer Vision and Pattern Recognition*, 2017. 1, 2
- [46] Simon Niklaus, Long Mai, and Feng Liu. Video Frame Interpolation via Adaptive Separable Convolution. In *IEEE International Conference on Computer Vision*, 2017. 1, 2, 7, 8
- [47] Simon Niklaus, Long Mai, and Oliver Wang. Revisiting Adaptive Convolutions for Video Frame Interpolation. In *IEEE Winter Conference on Applications of Computer Vision*, 2021. 2, 7, 8
- [48] Simon Niklaus, Xuaner Cecilia Zhang, Jonathan T. Barron, Neal Wadhwa, Rahul Garg, Feng Liu, and Tianfan Xue. Learned Dual-View Reflection Removal. In *IEEE Winter Conference on Applications of Computer Vision*, 2021. 1
- [49] Avinash Paliwal and Nima Khademi Kalantari. Deep Slow Motion Video Reconstruction With Hybrid Imaging System. *IEEE Transactions on Pattern Analysis and Machine Intelligence*, 42(7):1557–1569, 2020. 2
- [50] Junheum Park, Keunsoo Ko, Chul Lee, and Chang-Su Kim. BMBC: Bilateral Motion Estimation With Bilateral Cost Volume for Video Interpolation. In *European Conference on Computer Vision*, 2020. 2, 7, 8
- [51] Junheum Park, Chul Lee, and Chang-Su Kim. Asymmetric Bilateral Motion Estimation for Video Frame Interpolation. In *IEEE International Conference on Computer Vision*, 2021. 2, 7, 8
- [52] Tomer Peleg, Pablo Szekely, Doron Sabo, and Omry Sendik. IM-Net for High Resolution Video Frame Interpolation. In *IEEE Conference on Computer Vision and Pattern Recognition*, 2019. 2
- [53] Fitsum A. Reda, Deqing Sun, Aysegül Dundar, Mohammad Shoeybi, Guilin Liu, Kevin J. Shih, Andrew Tao, Jan Kautz, and Bryan Catanzaro. Unsupervised Video Interpolation Using Cycle Consistency. In *IEEE International Conference on Computer Vision*, 2019. 2
- [54] Jonathan Shade, Steven J. Gortler, Li wei He, and Richard Szeliski. Layered Depth Images. In *Conference on Computer Graphics and Interactive Techniques*, 1998. 2
- [55] Wang Shen, Wenbo Bao, Guangtao Zhai, Li Chen, Xiongkuo Min, and Zhiyong Gao. Blurry Video Frame Interpolation. In *IEEE Conference on Computer Vision and Pattern Recognition*, 2020. 2
- [56] Zhihao Shi, Xiaohong Liu, Kangdi Shi, Linhui Dai, and Jun Chen. Video Interpolation via Generalized Deformable Convolution. *arXiv/2008.10680*, 2020. 2
- [57] Hyeonjun Sim, Jihyong Oh, and Munchurl Kim. XVFI: eXtreme Video Frame Interpolation. In *IEEE International Conference on Computer Vision*, 2021. 2, 7, 8
- [58] Deqing Sun, Xiaodong Yang, Ming-Yu Liu, and Jan Kautz. PWC-Net: CNNs for Optical Flow Using Pyramid, Warping, and Cost Volume. In *IEEE Conference on Computer Vision and Pattern Recognition*, 2018. 5, 6
- [59] Zachary Teed and Jia Deng. RAFT: Recurrent All-Pairs Field Transforms for Optical Flow. In *European Conference on Computer Vision*, 2020. 6
- [60] Stepan Tulyakov, Daniel Gehrig, Stamatios Georgoulis, Julius Erbach, Mathias Gehrig, Yuanyou Li, and Davide Scaramuzza. Time Lens: Event-Based Video Frame Interpolation. In *IEEE Conference on Computer Vision and Pattern Recognition*, 2021. 2
- [61] Yang Wang, Haibin Huang, Chuan Wang, Tong He, Jue Wang, and Minh Hoai. GIF2Video: Color Dequantization and Temporal Interpolation of GIF Images. In *IEEE Conference on Computer Vision and Pattern Recognition*, 2019. 2
- [62] Zihao W. Wang, Weixin Jiang, Kuan He, Boxin Shi, Aggelos K. Katsaggelos, and Oliver Cossairt. Event-Driven Video Frame Synthesis. In *ICCV Workshops*, 2019. 2
- [63] Chao-Yuan Wu, Nayan Singhal, and Philipp Krähenbühl. Video Compression Through Image Interpolation. In *European Conference on Computer Vision*, 2018. 1

- [64] Xiaoyu Xiang, Yapeng Tian, Yulun Zhang, Yun Fu, Jan P. Allebach, and Chenliang Xu. Zooming Slow-Mo: Fast and Accurate One-Stage Space-Time Video Super-Resolution. In *IEEE Conference on Computer Vision and Pattern Recognition*, 2020. [2](#)
- [65] Xiangyu Xu, Li Si-Yao, Wenxiu Sun, Qian Yin, and Ming-Hsuan Yang. Quadratic Video Interpolation. In *Advances in Neural Information Processing Systems*, 2019. [2](#)
- [66] Tianfan Xue, Baian Chen, Jiajun Wu, Donglai Wei, and William T. Freeman. Video Enhancement With Task-Oriented Flow. *International Journal of Computer Vision*, 127(8):1106–1125, 2019. [2](#), [3](#), [5](#), [6](#), [7](#)
- [67] Zhiyang Yu, Yu Zhang, Deyuan Liu, Dongqing Zou, Xijun Chen, Yebin Liu, and Jimmy S. Ren. Training Weakly Supervised Video Frame Interpolation With Events. In *IEEE International Conference on Computer Vision*, 2021. [2](#)
- [68] Liangzhe Yuan, Yibo Chen, Hantian Liu, Tao Kong, and Jianbo Shi. Zoom-in-to-Check: Boosting Video Interpolation via Instance-Level Discrimination. In *IEEE Conference on Computer Vision and Pattern Recognition*, 2019. [2](#)
- [69] Haoxian Zhang, Yang Zhao, and Ronggang Wang. A Flexible Recurrent Residual Pyramid Network for Video Frame Interpolation. In *European Conference on Computer Vision*, 2020. [2](#)
- [70] Lili Zhao, Zezhi Zhu, Xuhu Lin, Xuezhou Guo, Qian Yin, Wenyi Wang, and Jianwen Chen. RAI-Net: Range-Adaptive LiDAR Point Cloud Frame Interpolation Network. *arXiv/2106.00496*, 2021. [3](#)
- [71] C. Lawrence Zitnick, Sing Bing Kang, Matthew Uyttendaele, Simon A. J. Winder, and Richard Szeliski. High-Quality Video View Interpolation Using a Layered Representation. *ACM Transactions on Graphics*, 23(3):600–608, 2004. [2](#)